Journal of Visualization, Vol. 9, No. 3 (2006)247-255

Continuous Scanning, Laser Imaging Velocimetry

Fincham, A. M.*[1, 2]

*1 Department of Aerospace and Mechanical Engineering, University of Southern California, Los Angeles, California 90089-1191, USA. E mail: afincham@usc.edu
*2 Laboratoire des Ecoulements Géophysiques et Industriels (LEGI), CNRS-UJF-INPG, Grenoble, France.

Received 2 December 2005
Revised 22 February 2006

Abstract : Careful exploitation of the anisotropy native to late time stratified and rotating flows permits the use of a laser scanning measurement technique to simultaneously resolve the 2D velocity field in O(100) slices. The technique relies on getting the Reynolds number from the length scale while keeping the velocity small, this provides a characteristic time scale that is sufficiently large to permit full 3D scanning through the measurement volume in a relatively short time. As the vertical velocity component of these late time stratified flows is effectively zero, all components of the deformation tensor are resolved. 3D, time resolved measurements of the vorticity and enstrophy fields associated with stratified rotating flows such as vortex dipoles, monopoles and wakes are presented.

Keywords : PIV, 3D, Scanning, Stratified, CIV.

1. Introduction

Particle Imaging Velocimetry techniques, Adrian (1991), Westerweel (1993), Grant (1994), Fincham and Spedding (1997), have been extensively used for two-dimensional measurements. Recent commercially driven advances in PC and camera technology allow for low cost continuous acquisition of high-resolution images. This opens up the possibility of using 3D scanning systems to resolve the velocity field in 3D space, without resorting to expensive, complicated and limited holographic recording systems, which due to their photographic nature can only capture a single time-step. Here we present a novel 3D time resolved measurement technique that differs from other scanning techniques in that the scanning process is continuous and the fluid volume is scanned multiple times for each measurement. Classical 3D scanning techniques involve acquiring many parallel slices within a given volume and subsequently reconstructing the flow-field within. Clearly this acquisition must be done in a time that is short compared to the fastest eddy turn over time of importance within the volume. This opens up two different approaches to making such measurements, first, to achieve the fastest possible image acquisition rate; second, to have the longest possible eddy turn over time of the structures of interest. As the eddy turnover time L/U (where L represents a typical eddy diameter and U its characteristic velocity) is inversely proportional to the velocity, we should aim to get our Reynolds number UL/υ from the length scale and not the velocity scale. The strong anisotropy present in late time stratified flows proves to be a distinct advantage for the application of this technique and can be exploited as in the 2D measurements of stratified grid turbulence, Fincham et al. (1996). In these flows seeding particles reside for long times (indefinitely) in the same horizontal plane, reliving the constraint in measurable Reynolds number imposed by particles leaving the light sheet in an isotropic flow, Fincham and Spedding (1997). In the experiments discussed here, we are again helped by the nature of stratified/rotating flows which behave in a quasi two-dimensional

manner, exhibiting inverse energy cascade phenomenon where energy accumulates at low wave-numbers (eddies with relatively large turnover times).

2. Measurements

2.1 Laboratory System

These experiments were performed on the Coriolis rotating platform in Grenoble, France. The platform is fitted with a 13-meter diameter by 1.2-meter deep circular tank. The platform is capable of making a full revolution in less than 20 seconds and the axis of rotation is better than 10^{-6} radians from vertical. Volumetric pumping systems permit the creation of arbitrary vertical density profiles using common salt. Making IV (Imaging Velocimetry) measurements in such a large facility poses specific problems, for example, the selection of suitable particles and the creation of a uniform laser light sheet for such large surfaces, see Fincham (1997), Fincham and Didelle (1998), for some technical discussion of the operation of the 3D optical measurement system at the Coriolis facility. Experiments in such a large tank require significant technical support but can provide many advantages over small tank experiments, apart from the larger Reynolds numbers obtained, low Rossby numbers ($R_o = U/Lf$, where f is the coriolis frequency)) can be obtained at modest rotation rates, reducing the undesirable centrifugal force that deforms the free surface. Often in smaller tanks, the time of observation is limited and can be too short for the development of certain instabilities. Additionally, the entire measurement system including the personnel, all work in the rotating frame, making the implementation of the experiment much the same as in the non-rotating case. Here, it is the large size that permits the creation of slowly moving vortices of significant Reynolds number that are susceptible to full 3D measurement.

The fluid is seeded with 700-micron diameter polystyrene beads that are carefully prepared by cooking and consecutive density separations to have a flat distribution of densities matching that of the linear salt-water stratification. Coherent light originating from a 5 watt Argon laser is passed into an optical fiber, the other end of which is attached to a small optical assembly that moves horizontally on a linear bearing traverse. Directly beneath the traverse, in the water, is a large 45° inclined mirror. A stepper motor controls the motion of the optical assembly, which consists of a small oscillating mirror driven in phase with the camera. The oscillating mirror creates a vertical sheet of laser light that passes through a thin glass plate held parallel to and just touching the surface of the water above the 45° mirror. In this way, horizontal motion of the optical assembly above the water translates directly into vertical motion of the laser sheet within the fluid, see Fig 1. The camera is fixed 5.5 meters above the water surface and a 25 mm f1.2 lens is used for the imaging. This provides a depth of field that is just sufficient to capture the volume of interest and any blurring is limited to the upper and lower slices, which are usually far from the structures of interest.

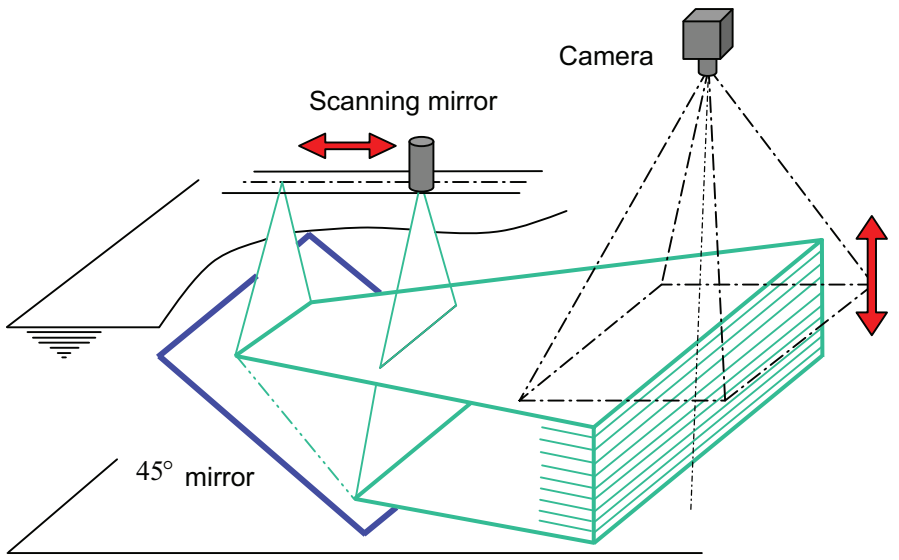

Fig. 1. Schematic diagram of the opto-mechanical scanning system.

2.2 Image Acquisition and Processing

Images were acquired directly to PC RAM with either a Pulnix 9701 camera running in digital output mode (768 x 484 pixels) at 30 fps 8 bits or with a SMD 1M60 at 512 x 512 or 1024 x 1024 pixel running at 110 or 60 fps respectively in 12 bits. Imaging Technology IC-PCI interface cards with AM-DIG16 and MTD type modules were used to interface the respective cameras. The SMD 1M60 was interfaced to a duel PCI bus 4-processor computer with 2 IC-PCI-MTD cards, this was necessary as this camera has a data output rate of 160 MB/sec, more than the theoretical limit for the 33 Mhz PCI bus available at the time. High quality digital output Interline and Frame-transfer CCD cameras are now available in 1024 by 1024 pixel format at 8-12 bits and up to 100 frames per second (newer CMOS sensor cameras working at over 3000 fps are just now becoming *affordable*). Again, large slowly moving vortices will be the easiest to measure given the constraints in the available imaging hardware.

The volume scan process proceeds as follows. An initial scan through all depths is made with continuous image acquisition to memory. During the acquisition stage the light sheet continues to move, and actually scans out a horizontal slab slightly thicker than the sheet itself, this ensures that no particles escape the sheet and avoids the need to intermittently stop the scanning, a process sure to introduce vibrations and greatly increase the scan times. On completion of the first scan, the light sheet is then quickly returned to the starting position. After the appropriate time interval the scan process is repeated to acquire the second image volume. This ensures a constant time interval between corresponding slices in each volume scan. Typical scan times produce time intervals between image pairs of between 2 and 4 seconds, though long by planar PIV standards, the vortices have time scales of O(100) seconds and good correlations between matching slices are achieved. The actual inter-scan time is determined by the pixel displacement that results in minimal error. As each slice measured may have its own characteristic velocity, it is not possible to minimize errors in all slices with just 2 scans, hence, a third or fourth scan of each volume is made to better resolve the weakly energetic planes. This multiple scan process is automatically repeated at pre-determined time intervals. Images from each slice are treated as described in Fincham and Spedding (1997) and Fincham and Delerce (2000). The resulting vector fields are combined into a 3D cube that is fit with a 3D 4th order tensor product spline, providing all derivatives of the horizontal velocity. With the assumption of $w \cong 0$, all components of the deformation tensor are resolved, yielding the 3 components of the vorticity vector. Stratified flows exhibit strong anisotropy with vertical scales being much smaller than the horizontal scales, for this reason we can assume that *dw/dx* and *dw/dy* are smaller than *dw/dz*. Although *w* is not measured, *dw/dz* is evaluated directly from the continuity equation and found to be small when compared to the other measured gradients, this allows us to ignore the contribution of *dw/dx* and *dw/dy* to the vorticity and certainly, to the enstrophy fields (which involves the square of these small gradients and is defined here as $1/2(\omega_x^2+\omega_y^2+\omega_z^2)$). Typical measurement conditions produce 80 x 80 x 80 independent vectors in volumes of about 200 x 200 x 60 cm^3. Due to the different distances of each slice from the stationary camera, different values of the pixels per centimeter scaling are required for each slice, this is done by linearly interpolating between a calibration of the upper and lower slice. The irregular grid so created is re-regularized in the spline interpolation process. Error analysis based on 2D simulations combined with checks on continuity and vertical light sheet measurements indicate that the errors in measured vorticity are about 5 %.

It is appropriate to briefly discuss the nature of decaying stratified flows here, as it is this property of the flow that makes these measurements possible. It is well known that an initially turbulent patch in a stably stratified fluid will eventually organize into one or more coherent quasi-2D vortices with negligible vertical velocity but strong horizontal vorticity. The process of *collapse* in a stratified fluid has been extensively studied, Hopfinger, (1987) and it is generally believed that in free decay, after about 20 buoyancy periods (based on the Brunt-Väisälä or buoyancy frequency *N*, defined as $N = \sqrt{-(g/\overline{\rho})\partial\rho_o/\partial z}$, where $\overline{\rho}$ is the mean density), the vertical velocity component is dominated by weak residual low wave-number internal wave motions. Clearly in the initial stages of collapse the assumption $w \cong 0$ is not valid but as the objective is to understand the dynamics of the late time quasi-2D vortices, we need not concern ourselves with the measurement of the collapse process itself. It suffices to note the initial conditions of the generation mechanism and wait until after the collapse to start the measurements. Typical velocities at the time of

measurement are on the order of several mm/sec, but due to the meter sized length scales Reynolds numbers are still O(10^3). An extension of this technique to full 3-component volumetric measurement, where the correlations are performed in three-dimensions, directly on the 3D image volume pairs, is described in Fincham (2003).

3. Results and Discussion

3.1 Stratified Dipole

Fluid of neutral buoyancy is injected horizontally through a tube of 17 mm diameter at the mid-depth of the stratified fluid. In the non-rotating case a quasi-2D dipolar vortex is formed that propagates away from the jet along its axis, individual horizontal sections reveal a relatively symmetric dipole that can be modeled as a Lamb-Chaplygin dipole, Flor and van Heijst (1994). The buoyancy frequency N= 0.04 rad/sec and the Reynolds number of the jet at exit is about O(10^3). An iso-surface of the vertical component of vorticity is shown in Fig. 2 (the vertical axis has been stretched by 3 throughout this paper), here the tubes of vertical vorticity are bent back behind the dipole due to the vertical variability in the propagation speed which must go to zero above and below the structure. Of particular interest is the actual enstrophy field, two views of which are shown in Fig. 3, along with some vortex filament trajectories. The complex form is due mainly to the horizontal components of vorticity that's composed entirely of *du/dz* and *dv/dz* terms. The enstrophy associated with the horizontal components of vorticity is typically 10 times stronger than that associated with the vertical component, Fincham et al. (1996). It is the vertical vorticity that controls the dynamics while the baroclinically stabilized horizontal vorticity is responsible for the dissipation of the structure. Examination of Fig. 3 shows low enstrophy regions in the center (necessary for symmetry) and 4 diagonally sloping holes that correspond approximately to the centers of rotation of the deformed vortex cores, this can be better seen in Fig. 4, which is a superposition of Figs. 2 and 3. It is the vertical coherence along the vortex cores that reduces *du/dz* creating local enstrophy minima. A detailed study of such dipoles using this technique can be found in Praud and Fincham (2005).

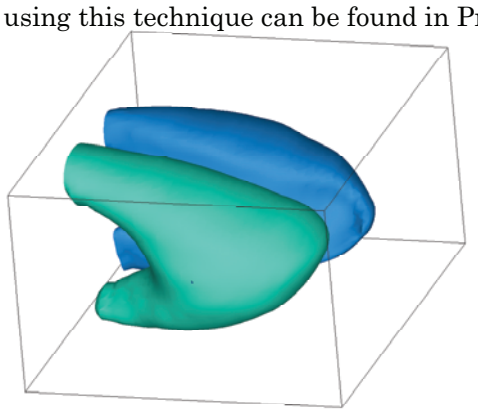

Fig. 2. Iso-surface of the vertical component of vorticity (10 % of maximum value), dipole is propagating to the right (note: to enhance the visualization the vertical axis has been stretched by a factor of 3 throughout this paper).

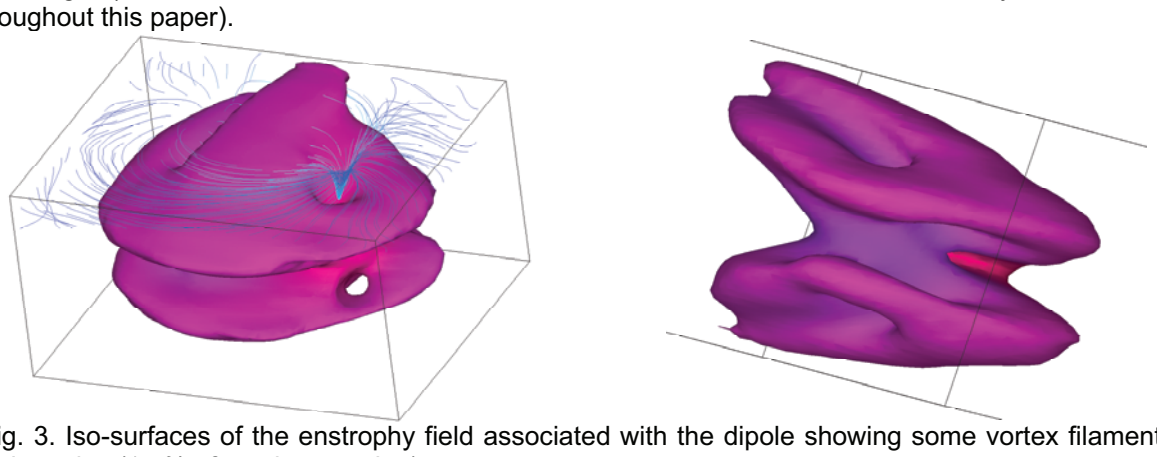

Fig. 3. Iso-surfaces of the enstrophy field associated with the dipole showing some vortex filament trajectories (15 % of maximum value).

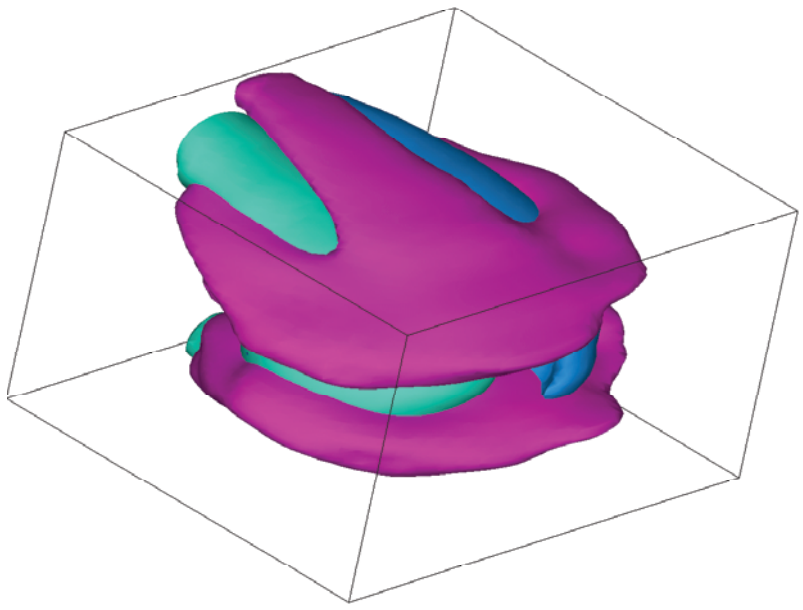

Fig. 4. Superposition of Figs. 2 and 3 showing locations of the vortex cores relative to the enstrophy structure.

3.2 Stratified Rotating Dipole

The dipole created by a similar jet in a rotating stratified fluid initially forms in the same way but quickly feels the Coriolis force and like any object moving in a anti-clockwise rotating frame, tends to veer to the right to conserve its angular momentum. This creates a competition with the symmetrically formed dipolar structure that wants to continue to propagate along a line parallel to the axis of the jet. The problem is resolved by the shedding of a cyclonic patch of vorticity by the dipolar structure, leaving an asymmetric dipole that now naturally turns to the right. The structure attempts to propagate in circles of Rossby radius $L_R = N\lambda/f$ where λ is the thickness of the structure and f the Coriolis parameter corresponding to twice the rotational speed of the tank. This can be seen in Fig. 5 where the vertical vorticity in the central slice of the volume is shown for different times.

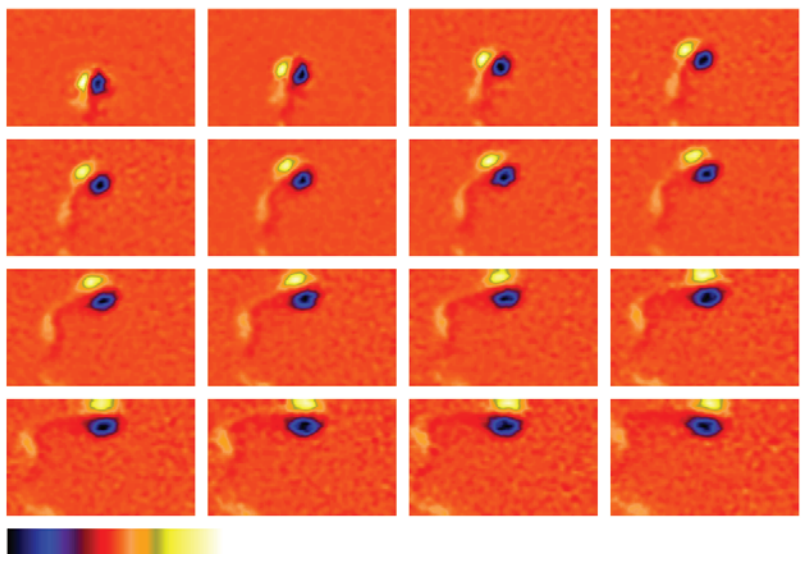

Fig. 5. Time evolution of the vertical component of vorticity for the central slice of the volume measurement, each panel has been normalized by the maximum value, orange is zero, blue/black is anticyclonic and yellow/white is cyclonic. The maximum vorticity values range from 0.1 - 0.03 Hz during this sequence.

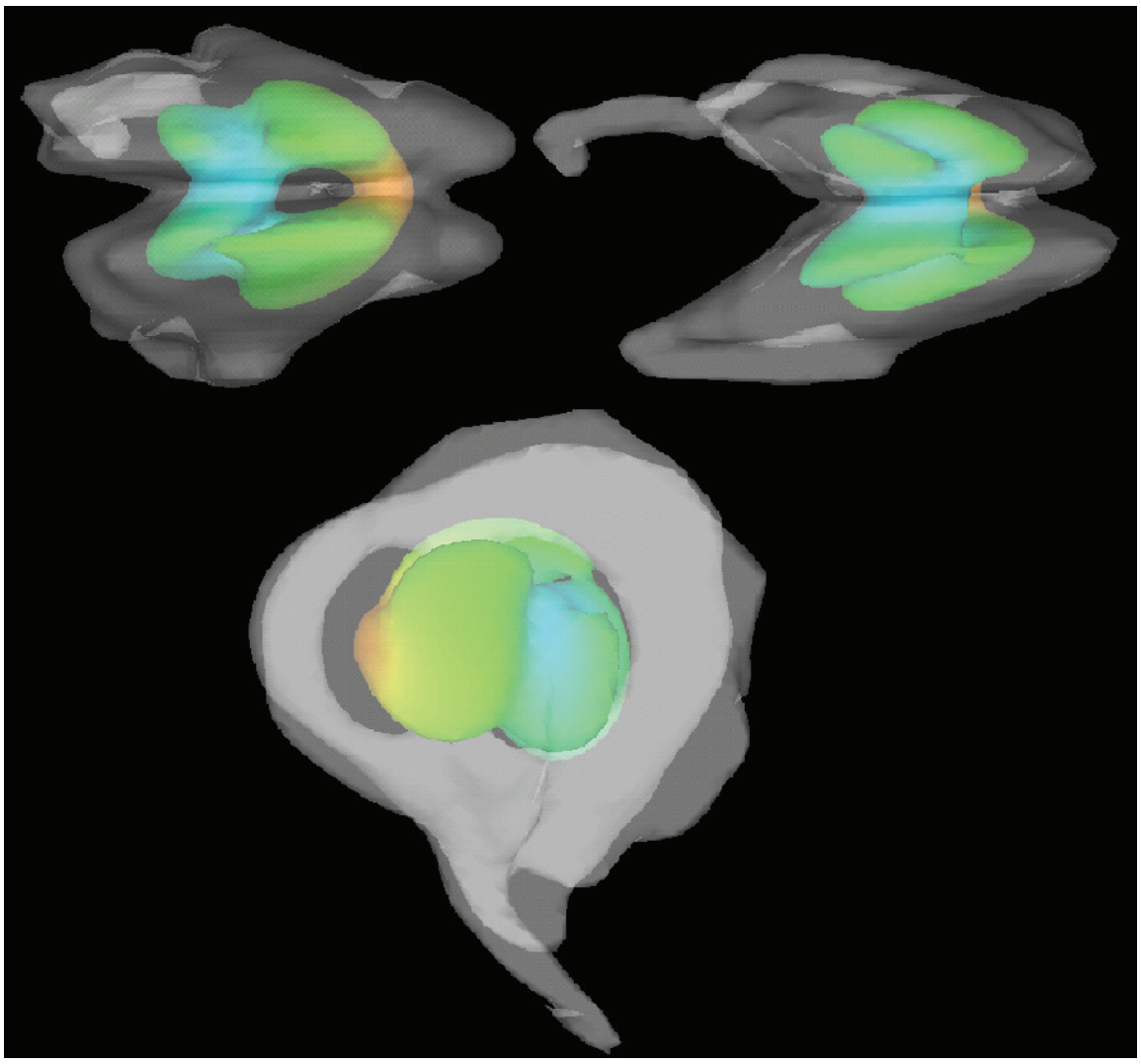

Fig. 6. Isosurfaces showing 3 views of the dipole with enstrophy thresholds of 15 and 50 %. Re ~ 1000, Ro ~ 0.15 and Fr ~ 0.015; from top left to right; frontal view, side view and plan view.

Three orthogonal views of the iso-enstrophy surface of the dipole after the detachment are shown in Fig. 6. Here a transparent surface corresponding to an enstrophy threshold of 15 % of the maximum value is shown together with a 50 % surface colored by the magnitude of the vertical component of vorticity. In the frontal view the rotation-induced asymmetry in the core is evident.

Fincham (2000), using this 15 % iso-enstrophy surface to define the dipolar structure, calculated the decay rate of the energy within this surface as a function of time. This global energy decay, *dE/dt,* was compared with the internal viscous dissipation of energy $2\upsilon S_{ij}S_{ij}$ calculated within the same volume for each instance in time. After 30 buoyancy periods the vortex decay is exactly accounted for by the measured deformation gradients. Such comparisons serve as reliable checks on the quality of the spatial derivatives obtained from such measurements.

3.3 Stratified Flat-Plate Wakes

The flow behind a vertical flat plate in a linearly stratified fluid exhibits interesting dynamics. The 2D nature of the flow generation (forcing) is quickly destroyed by the tendency for stratified fluids to form horizontal layers. The initial vorticity input is vertical but the columnar vortices so formed are susceptible to a "zig-zag" type instability, Billant and Chomaz (2000a,b), that vertically de-correlates the vortex cores generating horizontal vorticity and favoring the formation of layers. Figure 7(a) shows an iso-surface of the vertical component of vorticity for a Reynolds number of 335 based on the plate diameter. Note the vortices remain in phase with each other downstream of the plate. At

slightly higher Reynolds number the "zig-zag" develops much more rapidly and the vortices break into layers, see Fig. 7(b).

The effects of background rotation on this wake flow are to promote a vertical realignment of the vortices, this can be seen in Fig. 8 which shown the same flow as in Fig 7(a) but with background rotation corresponding to a Rossby number of 1.

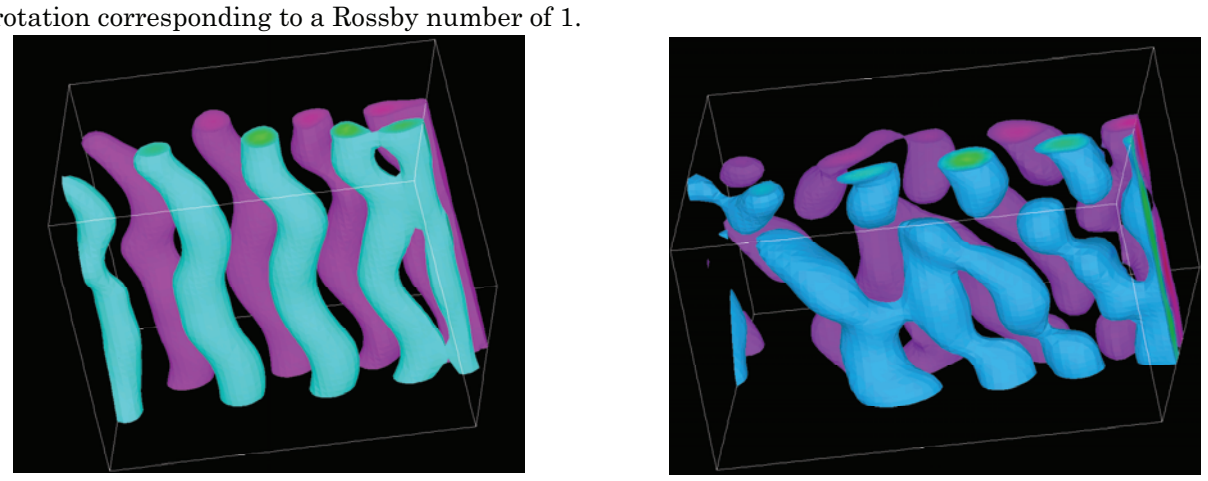

(a) (b)

Fig. 7. (a) Iso-surface of the vertical component of vorticity associated with the wake of a vertical flat plate in a stably stratified fluid Re = 335, Fr = 0.08. (b) Same for Re = 670, Fr = 0.16. The plate is towed from left to right and the vortices at the extreme right of the image (a) are still attached to the plate.

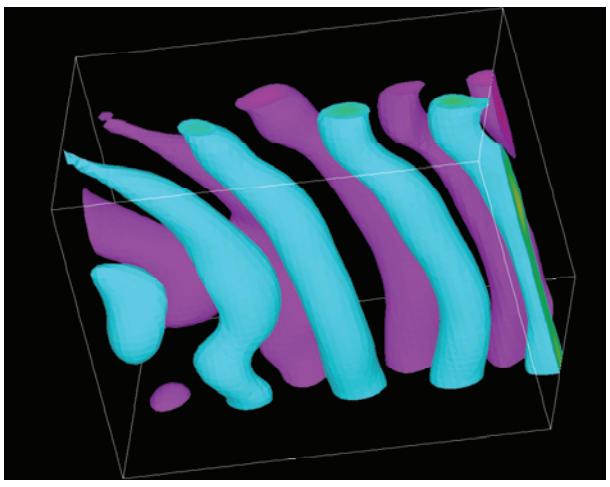

Fig. 8. Iso-surface of the vertical component of vorticity for same conditions as Fig. 7(a) but with background rotation corresponding to a Rossby number of 1.

3.4 Anticyclonic Lenses (Meddies)

Intermediate density fluid injected vertically at the mid depth into a linearly stratified rotating medium spreads out radially and starts to rotate anti-cyclonically due to the Coriolis force. These intermediate density lenses are similar to the Mediterranean eddies MEDDIES formed off cape St. Vincent by the Mediterranean outflow, Sadoux et al. (2000). Due to the relatively sharp density interface separating the injected fluid from the ambient fluid, there is significant refraction of the light sheet upon entering the lens. As a result, in-situ calibration of the light sheet position is required for proper reconstruction of these volumes. Figure 9(a) shows an iso-surface of the vertical component of vorticity, ω_z, for a typical stable anticyclonic lens formed from the slow injection of 10 liters of intermediate fluid. The anticyclonic core is surrounded by a torus of cyclonic vorticity, which has a shielding effect on the central plane. Although *shielded* in the 2D sense, these vortices are free to interact with other structures above and/or below. The enstrophy field for the same vortex is shown in Fig. 9(b), it consists of a double torus. The vortex filaments associated with this structure form a single closed torus.

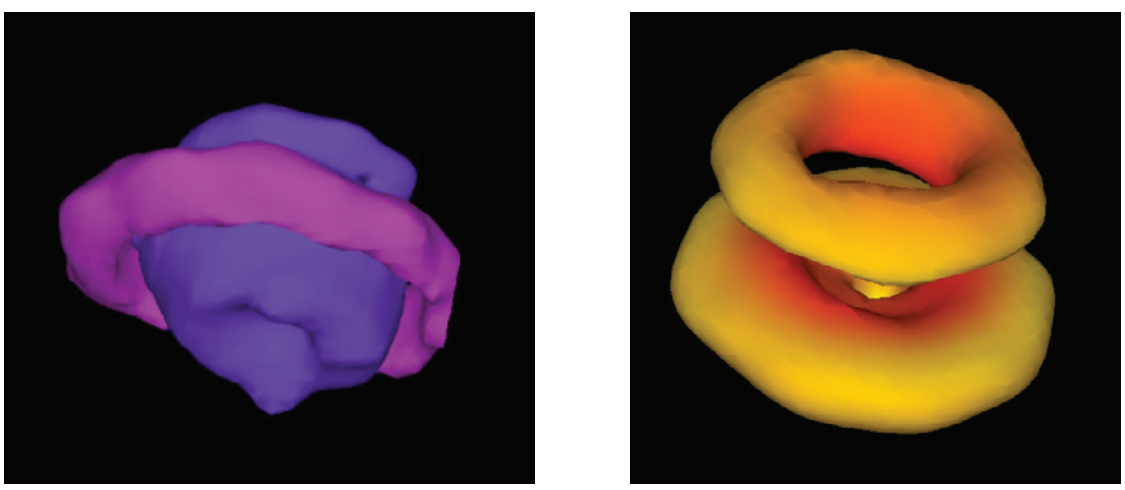

(a) (b)

Fig. 9. (a) Isosurface of the vertical component of vorticity for a stable anticyclonic lens vortex (meddie), (blue is anti-cyclonic vorticity, purple is cyclonic), (b) iso-enstrophy surface for same vortex.

When perturbed or at lower Rossby number these laboratory meddies can become baroclinically unstable, eventually breaking up to form multipolar structures. Figure 10 shows an unstable anti-cyclonic lens at 2 different times. The mushroom like structure in the center of Fig. 10(a) is a byproduct of the meddie generation process; it oscillates vertically, helping to destabilize the structure, which eventually breaks down to form a tripolar vortex (Fig. 10(b)).

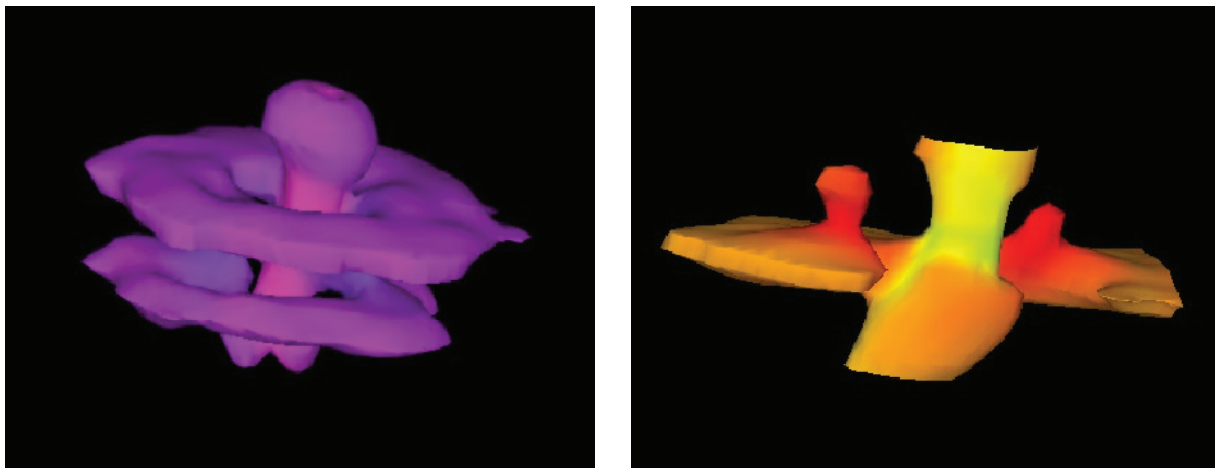

(a) (b)

Fig. 10. Iso-enstrophy surface of an unstable anti-cyclonic lens vortex at (a) early time and (b) after breakdown into tripole (the color represents the value of the vertical component of vorticity, for (b), yellow is anti-cyclonic and red is cyclonic).

4. Conclusion

Three dimensional, two component, time resolved measurements of complex vortex structures have been made. All significant components of the deformation tensor have been resolved. The measurement technique takes advantage of the anisotropy inherent to late time stably stratified and/or rotating flows but relies principally on the relatively long eddy turnover times associated with the vortices. Details of the 3D vortex topography reveled with this technique provide valuable incite into the mechanism of instability and interaction for a wide variety of flows. Such information could not be obtained from classical 2D IV techniques. Examples of more quantitative analysis using this technique on stratified turbulent flows at relatively large Reynolds numbers can be found in Praud,

Fincham and Sommeria (2005), Praud and Fincham (2005) and Praud, Sommeria and Fincham (2005).

Limitations of affordable imaging equipment have restricted this technique to large experimental facilities such as the Coriolis platform, where the Reynolds number is obtained from the length scale and the velocity is the order of several mm/sec. Current availability of high-speed digital imaging equipment will make this technique commonplace at smaller scale in the near future.

Acknowledgements

These laboratory simulations would not have been possible without the enthusiastic participation of both Dr. Henri Didelle and Mr. René Carcel. This work has been supported by the European Commission project HYDRIV, Contract HPRI-1999-50042.

References

Adrian, R. J., Particle-imaging techniques for experimental fluid mechanics, Ann. Rev. Fluid Mech., 23 (1991), 261-304.

Billant P. and Chomaz J-M., Experimental evidence for a new instability of a vertical columnar vortex pair in a strongly stratified fluid, *J. Fluid Mech.*, 418 (2000), 167-188.

Billant, P. and Chomaz, J-M., Theoretical analysis of the zigzag instability of a vertical columnar vortex pair in a strongly stratified fluid, J. Fluid Mech., 419 (2000), 29-63.

Fincham, A. M., Maxworthy, T. and Spedding, G. R., Energy dissipation and vortex structure in freely decaying, stratified grid turbulence, Dyn. Atmos. Oceans, 23 (1996), 155-169.

Fincham, A. M. and Spedding, G. R., Low-cost, high resolution DPIV for measurement in turbulent fluid flows, Experiments in Fluids, 23 (1997), 449-462.

Fincham, A. M. and Delerce, G., Advanced optimization of Correlation Imaging Velocimetry Algorithms, Experiments in Fluids, 29 (2000), S13-S22.

Fincham, A. M., 3D measurement of vortex structures in stratified fluid flows, Simulation and identification of organized structures in flows (eds. J. N. Soerensen, E. J. Hopfinger and N. Aubry), Proc. IUTAM Symp. (1997), 273-287, Kluwer.

Fincham, A. M. and Didelle, H., Experimental quantitative flow visualization using 3D DPIV, 8th International Symposium on Flow Visualization (Sorrento, Italy), (1998).

Fincham, A. M., Coherent vortex structures in stably stratified rotating fluids. IUTAM Symposium on Developments in Geophysical Turbulence (eds. R. M. Kerr and Y. Kimura), Kluwer series; Fluid Mechanics and its Applications, 58 (2000), 193-204.

Fincham, A. M., 3 component, volumetric, time-resolved Scanning Correlation Imaging Velocimetry, Proc. 5th Inter. Symp. on Particle Image Velocimetry (Busan, Korea), (2003), 2-16.

Flor, J. B. and van Heijst, G. J. F., An experimental study on dipolar structures in a stratified fluid, J. Fluid Mech., 279 (1994), 101-133.

Grant, I., Selected papers on Particle Image Velocimetry, SPIE Milestone Series, MS 99 SPIE, (1994), Washington.

Hopfinger, E. J., Turbulence in stratified fluids: a review, J. Geophys. Res., 92 (1987), 5287-5303.

Praud, O., Fincham, A. M. and Sommeria, J., Decaying grid turbulence in a strongly stratified fluid, J. Fluid Mech., 522 (2005), 1-33.

Praud, O. and Fincham, A. M., The structure and dynamics of stratified dipolar vortices, J. Fluid Mech., 544 (2005), 1-22.

Praud, O., Sommeria, J. and Fincham, A. M., Decaying grid turbulence in a rotating stratified fluid, J. Fluid Mech., 547 (2006), 389-412.

Sadoux, S., Baey, J-M., Fincham, A. M. and Renouard, D., Experimental study of the stability of an intermediate current and its interaction with a cape, Dyn. Atmos. Oceans, 31 (2000), 165-192.

Westerweel, J., Digital Particle Image Velocimetry Theory and Application, (1993), 235, Delft Univ. Press.

Author Profile

Adam Fincham: He received his Ph.D. in Aerospace Engineering (Geophysical Fluid Dynamics) in 1994 from the University of Southern California. He worked as Chargé de Recherche for the CNRS at LEGI, Universite Joseph-Fourier, Grenoble, France from 1995-2004, where he performed experiments on the large rotating platform, Coriolis. He currently works at the University of Southern California Department of Aerospace and Mechanical Engineering as an Associate Research Professor. His current research interests include, turbulence and vortex structures in stratified and/or rotating flows, advanced algorithms for DPIV, 3D Scanning Imaging Velocimetry, particle dynamics in turbulent flows with application to oceanic planktonic ecosystems and sonic boom interactions with the ocean surface.